engineering proceedings

MDPI

Proceeding Paper

In Vitro Antimicrobial and Anticancer Activity of Metallic Nanoparticles (Ag and FeO) against Human Pathogenic Bacteria and Cancer Cell Lines †

Shama Parveen [1], Vikas Gupta [1,*], Anuj Kandwal [2,*] and Veera Nagendra Kumar [3]

[1] Department of Chemistry, Faculty of Science, Motherhood University, Haridwar 247661, India; shamahussainktw@gmail.com
[2] Department of Chemistry, Faculty of Science, Harsh Vidya Mandir P.G. College, Raisi, Haridwar 247661, India
[3] Department of Zoology, Faculty of Science, Government College for Men (Autonomous), Kadapa 516004, India; veeranagendrakumar@gmail.com
* Correspondence: polyiftm1@gmail.com (V.G.); anujkandwal4@gmail.com (A.K.)
† Presented at the 4th International Electronic Conference on Applied Sciences, 27 October–10 November 2023; Available online: https://asec2023.sciforum.net/.

Abstract: The global health community is extremely concerned about the emergence and spread of antibiotic resistance as well as the evolution of new strains of disease-causing organisms. It takes the creation of novel pharmaceuticals or access to a supply of innovative therapeutics for a disease to be effectively treated. Commonly used medicinal herbs in our society could be a great source of medications to combat this issue. The antibacterial and anticancer capabilities of metallic nanoparticles made from plants are the main focus of this work. Two distinct nanoparticles were tested for their antibacterial and anticancer properties against four cancerous cell lines (prostate cancer, lung cancer A549, HeLa, and MCF-7) and five pathogenic microbes (*Staphylococcus aureus*, *Bacillus subtilis*, *Pseudomonas aeruginosa*, and *Escherichia coli*) bacteria, as well as one yeast (Candida albicans). Metallic nanoparticles from the plants *Leucas cephalotes* (AgNPs) and *Ajuga macrosperma* (FeONPs) were tested for their antibacterial capabilities using the agar well diffusion method and their ability to fight cancer using the MTS and MTT assays. According to the findings, AgNPs synthesized from *Leucas cephalotes* showed the strongest potential against *Pseudomonas aeruginosa* and *Staphylococcus aureus*. The zones of inhibition (ZOI) of *Leucas cephalotes*' AgNPs were 19 mm and 18 mm respectively. It was also discovered that the FeONPs of *Ajuga macrosperma* had the most potential against the MCF-7 cancer cell line. Prostate cancer and lung cancer (A549) cell lines were the ones that responded most favorably to the AgNPs of *Leucas cephalotes*.

Keywords: antimicrobial activity; anticancer cancer activity; silver nanoparticles; iron oxide nanoparticles

check for updates

Citation: Parveen, S.; Gupta, V.; Kandwal, A.; Kumar, V.N. In Vitro Antimicrobial and Anticancer Activity of Metallic Nanoparticles (Ag and FeO) against Human Pathogenic Bacteria and Cancer Cell Lines. *Eng. Proc.* **2023**, *56*, 294. https://doi.org/10.3390/ASEC2023-15910

Academic Editor: Manoj Gupta

Published: 7 November 2023

Copyright: © 2023 by the authors. Licensee MDPI, Basel, Switzerland. This article is an open access article distributed under the terms and conditions of the Creative Commons Attribution (CC BY) license (https://creativecommons.org/licenses/by/4.0/).

1. Introduction

Antibiotics are essential for managing infectious disorders and preventing infection during difficult surgeries such organ transplants, joint replacements, or heart surgeries. However, it is evident that overusing antibiotics starts the emergence of microbial resistance [1]. The length of hospital stays increases as a result of multidrug resistance to common infections, and fatality rates are also observed to rise. The need to research novel approaches to treating resistant bacteria results from this [2]. Cancer, which results in unchecked cell transformation, dynamic genome alteration, and the development of malignant characteristics in normal cells, was also found to promote resistance to chemotherapy, a frequent cancer treatment [3]. The difficulties encountered in cancer therapy nowadays lead to limitations in the management of cancer. Among them are the absence of an early diagnosis, nonspecific systemic distribution, insufficient drug concentrations reaching the

tumor, and an inability to track therapeutic outcomes. Medication delivery issues and medication retention at the target location are the root of serious consequences including multidrug resistance [3,4]. Technology may be able to provide answers to these existing cancer therapy roadblocks as well as to the problem of bacterial antibiotic resistance [5,6]. To be called "nanosized," a nanoparticle's size must fall between 1 and 100 nm [7]. Nanoscale is a field of science relating to the molecular scale regulation of substances. A material's chemical and physical characteristics change depending on its nanosize, ranging from those of larger substances or larger components. This has attracted attention among scientist because of its extensive variety of applications.

Biological techniques for synthesizing NPs using plant leaf extracts or organisms like fungi, bacteria, and algae are considered eco-friendly substitutes for chemical synthesis because such approaches are nontoxic and less cost- and energy-intensive [8]. Plant extract-based NP production approaches are more beneficial than environmentally-friendly biological approaches because cell cultures are not required [9]. Moreover, NP production using plants is beneficial because of the safe handling and easy availability associated with plants and their extensive metabolite content in facilitating reduction [10].

The main contributors to this phenomenon are a high surface area compared to volume ratio per unit, surface plasmon resonance (SPAR), intense reactivity to chemicals, stability, high catalytic efficiency, remarkable strength in mechanics, and decreased melting temperatures [11]. Metal salts can be reduced in a solution or atoms can be gathered together to create metal nanoparticles.

2. Materials and Methods

2.1. Chemicals and Biological Materials

Materials: Leaves of *Leucas cephalotes* and *Ajuga macrosperma*, *silver nitrate* ($AgNO_3$), copper sulphate, ferric sulphate, sodium hydroxide, distilled water. PC-3 (prostate cancer), HeLa, A549 lung cancer, and MCF-7 (breast cancer) cell lines. Gram-positive (*Staphylococcus aureus* and *Bacillus subtilis*) and Gram-negative (*Pseudomonas aeruginosa* and *Escherichia coli*) bacteria, as well as one yeast (*Candida albicans*) bacterial strain.

2.2. Collection of Plants

The leaves of the *Leucas cephalotes* and *Ajuga macrosperma* were obtained from the local forest in Kotdwara, Pauri Garhwal, India (June and September 2020).

2.3. Preparation of the Plants

Extraction: After being dusted off with tap water, the gathered leaves of *Leucas cephalotes* and *Ajuga macrosperma* were then rinsed with distilled water. A 500 mL beaker and a 1000 mL beaker containing 5 g and 7 g of leaves were combined with 150 mL, 300 mL, and 500 mL of sterile water that had been distilled. The combination was then heated for 120 min and allowed to cool to room temperature (30 °C). The prepared mixture was coarsely ground in an Indian Ken Star kitchen blender before being filtered with Whatman filter paper No. 1. The filtrate was used to create iron oxide and silver nanoparticles.

2.4. Synthesis of Nanoparticles

2.4.1. Synthesis of Silver Nanoparticles

The production of Ag-NPs required mixing the leaf extract with 60 mL of a 0.1 M solution of water of $AgNO_3$ and stirring the mixture for 60 min at 60 °C. The tint changed after being mixed with the reduction mixture from brown to a dark brown color after 1 hour, with reference to the control, which indicated that the confirmation was undertaken by UV-visible spectroscopy.

2.4.2. Synthesis of Iron Oxide Nanoparticles

These nanoparticles of iron oxide were produced by combining one gram of ferric sulphate with 50 milliliters of water that had been deionized, and stirring the mixture at

80 °C for 15 min. After being heated on the magnetic stirrer for 2 h, the mixture of 50 mL of the $FeSO_4$ mixture and 12 mL of the *Ajuga macrosperma* leaf extract. The NP liquid's new coloration was a reddish brown at the same temperature.

2.5. Characterization

Characterization of Silver and Iron Oxide Nanoparticles

The absorbance of pure NPs was measured using an ultraviolet (UV)-visible spectrophotometer (Bio-spectrophotometer BL 198, ELICO Ltd., Delhi, India) in order to initially confirm the formation of NPs. The NPs' shape was determined using a scanning electron microscope (JEOL2100F). X-ray diffraction was used to investigate the nanoparticles' crystal structure. X-ray diffractometers with Cu-K radiations in the 2° range of 5° to 80° (Bruker Nano D8 ADVANCE, GmbH, Bremen, Germany) were used to obtain the X-ray diffraction (XRD) pattern. The zeta potential of NPs (Malvern Instruments Ltd., Malvern, UK) was measured in the range of −200 mV to 200 mV at 25 °C, using a count rate of 189.8 Kcps, to determine the stability of the system. A Fourier-transform infrared spectrophotometer (Microscope with Vertex 80 FTIR System, Bruker, Bremen, Germany) was used for the analysis, which covered the wavelength range from 4000 to 400 cm^1.

2.6. Antimicrobial Activity

2.6.1. Method

E. coli, *Staphylococcus aureus*, *Bacillus subtilis*, *Pseudomonas aeruginosa*, and *Candida albicans* were the MDR clinical isolates that were inoculated into Mueller Hinton broth. The culture was kept at 37 °C until the absorbance at 600 nm reached 0.8 O.D. (8 McFarland's standard). To assess the antibacterial potential of AgNPs and FeONPs, the agar well diffusion method was used with various modifications. Molten soft agar was mixed with one milliliter of 0.5 McFarland inoculum, then the mixture was put onto basal agar plates and allowed to set. With the aid of a cork borer, 6 mm wells in soft agar were bored, and 20 L of hour were added. The wells were then incubated at 37 °C for 24 h. We measured the zone of inhibition (Table 1).

Table 1. The inhibition zones for nanoparticles of silver and iron oxide produced using the agar well diffusion method.

S.N.	Sample Name	Bacteria Name	Zone of Inhibition
1.	AgNPs	*S. aureus*	18
		B. Subtilis	12
		E. coli	12
		P. aeruginosa	19
		Candida albicans	16
2.	ZnONPs	*S. aureus*	17
		B. Subtilis	NI
		E. coli	12
		P. aeruginosa	NI
		Candida albicans	NI

2.6.2. Cell Cytotoxicity

The PC3, A549 human lung cancer cell line, MCF-7, and HeLa with slight modification were employed in studies on cell cytotoxicity. The MTT and MTS (3-(4,5-dimethylthiazol-2-yl)-5-(3-carboxymethoxyphenyl)-2-(4-sulphonyl)-2H-tetrazolium) assays were applied to determine the state of health of the cells. Succinate dehydrogenase enzymes reduced MTT in the mitochondria of metabolically active cells, producing reducing equivalents like NADH and NADPH. A crystal of purple formazan that is insoluble was created. A spectrophotometer was used to measure the crystal after it had been solubilized in DMSO. In 96-well culture plates, 5000 A549 cells per well were seeded and cultured for 24 h in RPMI-1640 culture media. After being seeded for 24 h, the cells were exposed to AgNP,

CuONPs, and FeONPs that had been biologically produced at concentrations of 100, 200, 400, 600, and 800 g/mL for 48 h, with 50 M fisetin serving as a positive control. Fresh 100 L of 5 mg/mL of MTT solution was introduced to each well after 48 h, and each well was subsequently incubated for 3 to 4 h at 37 °C in a CO_2 incubator. The 100 L of DMSO was added after the MTT solution had been taken out. For the disintegration of the formazan crystals, the solution was left in the sterilizer for 15 min.

Thermo Scientific's Varioskan Flash microplate reader was used to read the plates at 570 nm following a brief premixing step. The method used to determine the percentage of viable cells is as follows: percentage of viable cells = average absorbance by treatment sample/average absorbance by control sample multiplied by 100.

3. Result and Discussion

In the present study, plant-mediated silver and iron oxide nanoparticles were explored by using silver nitrate and ferric sulphate as a reducing agent. The reaction mixture turned from colorless to brown and dark brown, which is the preliminary indication of the synthesis of AgNPs and FeONPs. It was confirmed by UV analysis.

3.1. Spectra of AgNPs and FeONP

3.1.1. UV-Visible

The technique of ultraviolet-visible spectroscopy is often employed to describe nanoparticles. The recognizable absorption in the visible range is caused by the metallic nanoparticles' surface plasmon resonance. Utilizing the 200–800 nm UV-visible spectrum, the absorbed energy of NPs was calculated. The absorbance at 432 and 218 nm, which is specific to silver and iron oxide nanoparticles, was observed, as can be seen in Figure 1a and relates to previous literature [12,13]. In an aqueous solution, silver and iron oxide nanoparticles have a brownish-yellow and red hue.

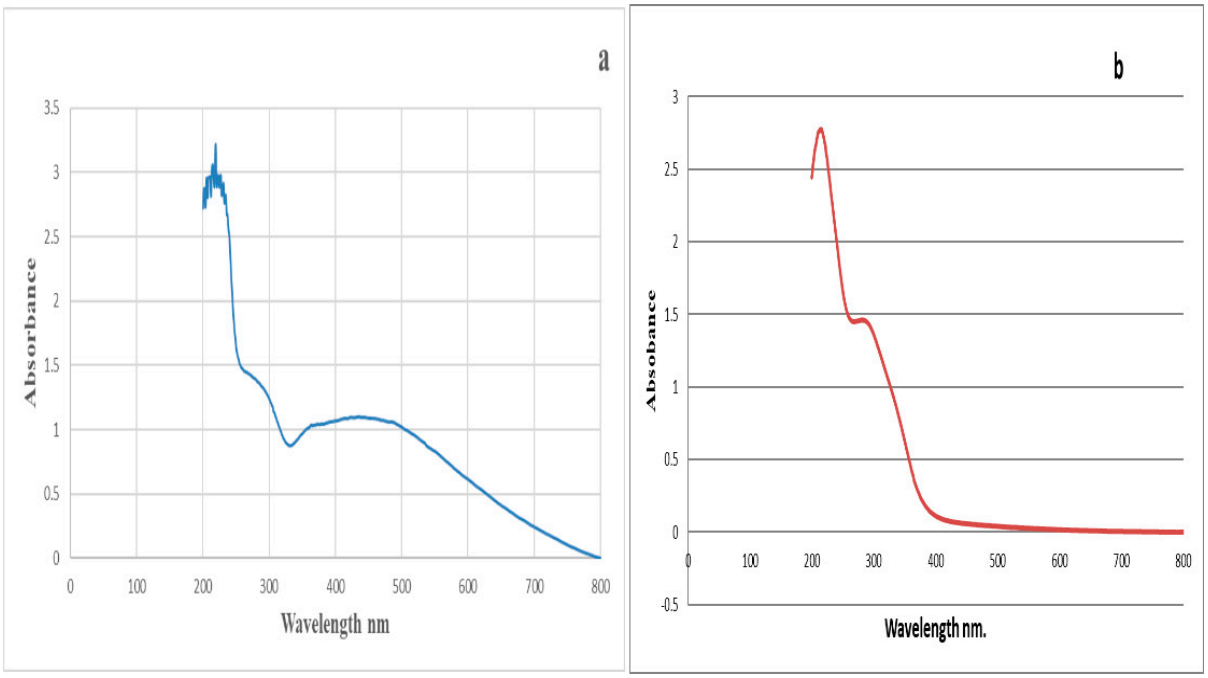

Figure 1. UV-visible spectra (**a**) AgNP spectra using *Leucas cephalotes* leaf extract. (**b**) FeONP spectra using *Ajuga macrosperma* leaf extract.

3.1.2. XRD

The diffraction intensities ranged between 20 to 80, and strong Bragg reflections were observed at 38.45, 44.28, 64.20, and 78.08, respectively, which is indexable by the facets of

AgNPs' fcc crystalline makeup, and which correspond to the planes of (111), (200), (220), and (311). It was discovered that the usual AgNP pattern produced by green syntheses had an FCC structure. Miller indices were found at (101), (221), and (200), coupled with the diffraction peaks at 11.62, 16.49, and 31.28. The standard data (JPCDS-01-079-1973) matched with synthesized FeoNP data (Figure 2). These data indicate that these diffraction spikes point to a body center cubic (BBC) configuration. [14]. Using the Debye Scherrer equation, it was possible to evaluate the silver an iron oxide nanoparticles' typical particle size. The average crystalline sizes of AgNPs and FeONPs were 24 and 37 nm, respectively.

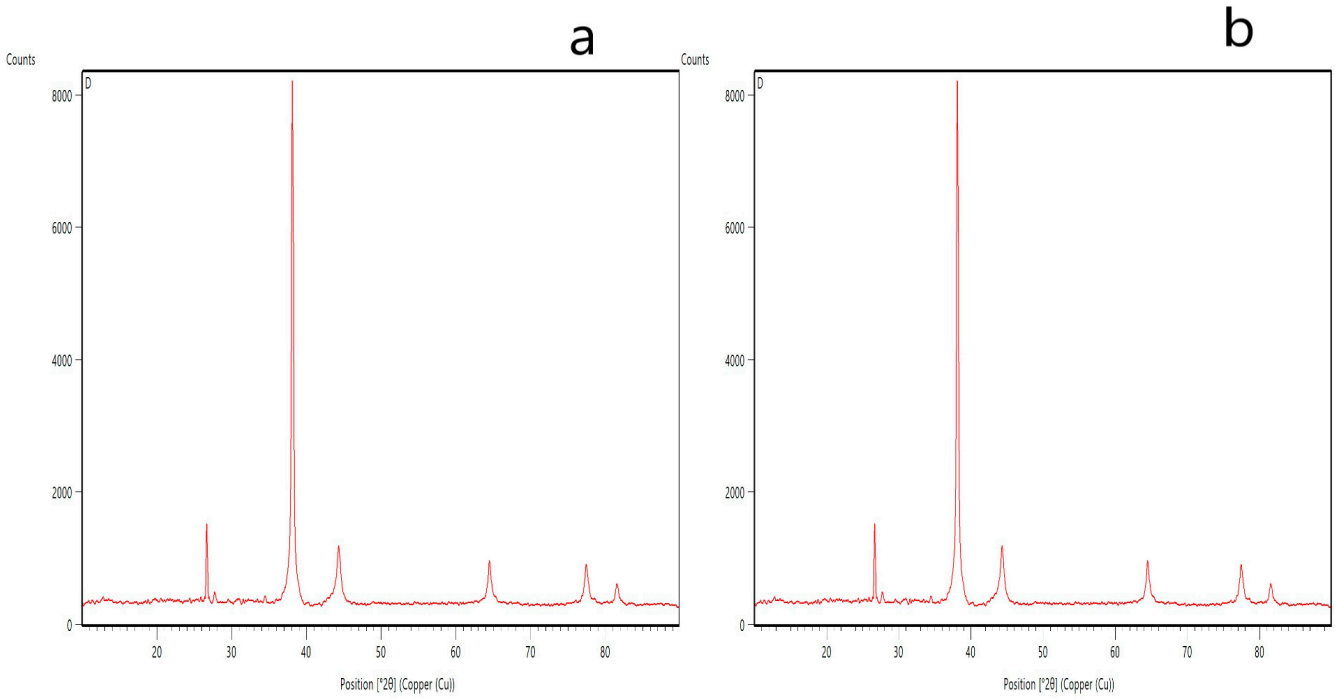

Figure 2. XRD spectra (**a**) AgNP spectra using *Leucas cephalotes* leaf extract. (**b**) FeONP spectra using *Ajuga macrosperma* leaf extract.

3.1.3. FTIR

Biogenic synthesis of silver and iron oxide nanoparticles utilized the plant extract as the reducing and capping agent. The FTIR analysis revealed groups involved in the reducing and capping agent, that is, groups preventing the aggregation of silver and iron oxide nanoparticles. By comparing the FTIR (Figure 3a,b) of AgNPs and FeONPs. The FT-IR spectra of AgNPs made by *Leucas cephalotes* leaf extract shows. The FTIR spectra showed numerous distinct bands about 3736, 2308, 1691, 1556, 902, 682, and 418 cm^1. The hydroxyl (O-H) functional group of polyphenolic species had a stretching vibration that had an absorption peak at 3736.12 cm^1. The peaks at 1691 and 2308 cm^{-1} were probably the result of the carbonyl (C=O) vibratory stretching originating from highly conjugated systems. In accordance with the Ag nanoparticles, peaks at 682 and 410 were located. The FTIR spectra for synthesized iron oxide nanoparticles revealed multiple distinct bands, at 3738.05 cm^{-1} and 3633.89 cm^{-1}, showing stretching vibrations of the -O-H functional group. The peak in absorption at 2306 cm^{-1} indicated the presence of the functional group (C-O). The signal detected at 1687 cm^{-1} may be due to carbonyl (C=O) stretching vibrations generated by highly conjugated systems. The prominence at 1068 cm^{-1} might serve as a representation of the (C-H) functional group.

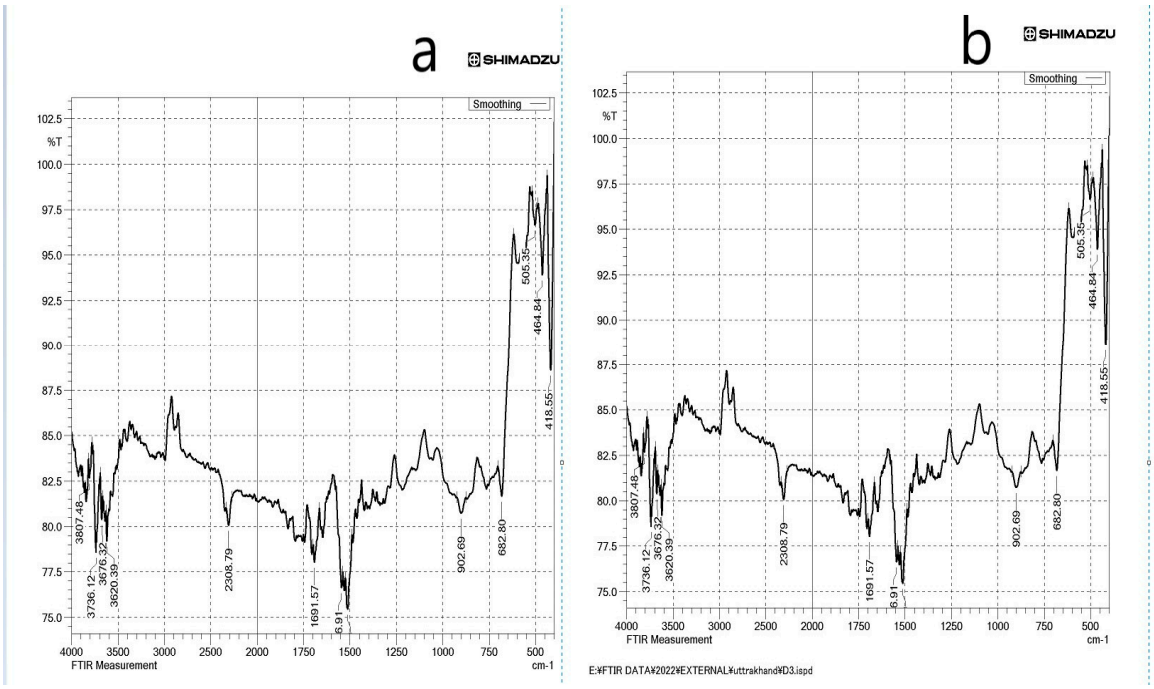

Figure 3. FTIR spectra (**a**) AgNP spectra using *Leucas cephalotes* leaf extract. (**b**) FeONP spectra using *Ajuga macrosperma* leaf extract.

3.2. Zeta Potential

The zeta potential was determined in order to explore the solution's colloidal stability. The term "zeta potential" refers to the electric potential of the particles at the double layer's interface. The microscopic particles are stable due to the surface charge covering them, which also inhibits agglomeration. According to Figure 4a,b, NPs have a zeta potential of −23.36, and −27.06 mV, correspondingly. This reading demonstrates the NPs' stability.

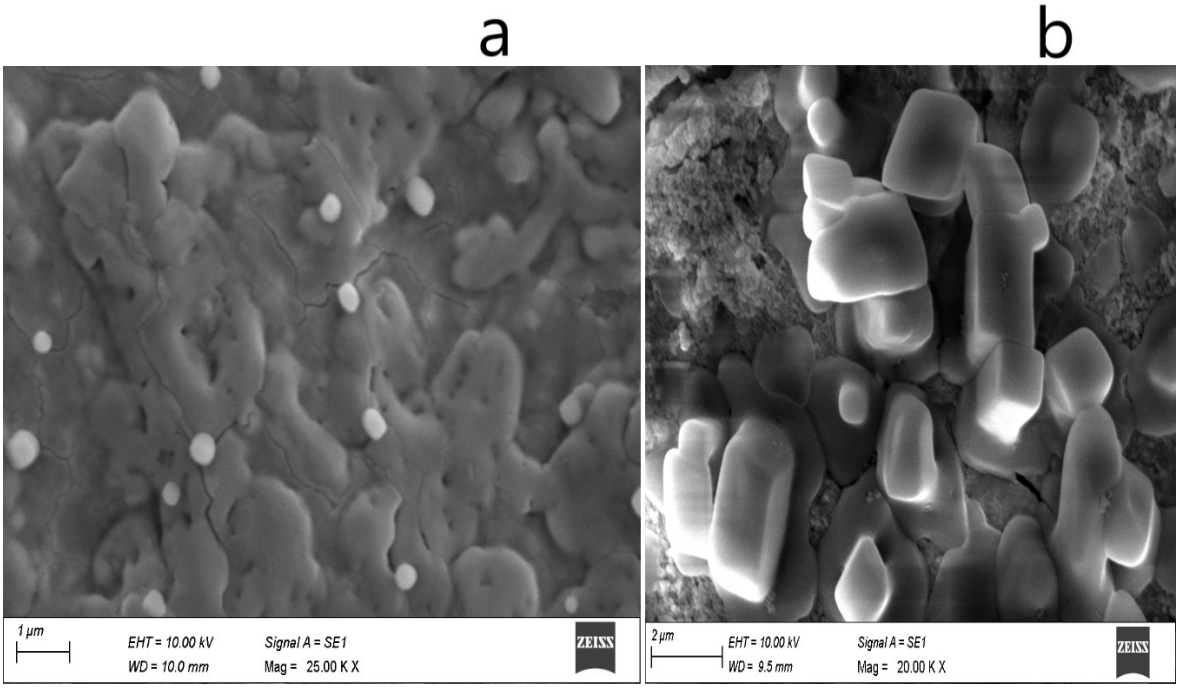

Figure 4. Morphology: (**a**) SEM image of AgNPs (**b**) SEM image of FeONPs.

3.3. Morphology

SEM with EDX

Using the electron micrograph of the complex as a starting point, the SEM was able to examine the skeletal anatomy of the synthesized AgNPs and FeONPs. The NPs' predominant shape was demonstrated to be spherical and cubic. According to the study, SEM photos demonstrated the spherical shape and size of the AgNPs produced by *Leucas cehalotes*, which were in the a wavelength ranging from 10 to 100 nm [15]. A similar outcome for AgNPs was reported according to Figures 4a, 5a and 6a, which depicted a 2 m with a magnification of 20 KX using Figures 4b, 5b and 6b, which depict the 1 m with 25.000 KX magnification. Imaging at higher magnifications was performed using FESEM. As indicated in Figure 4a,b, iron oxide nanoparticles made with *Ajuga macrosperma* leaf extract had a cube form and a selection of sizes of 5–27 nm. Similar results have previously been reported [16].

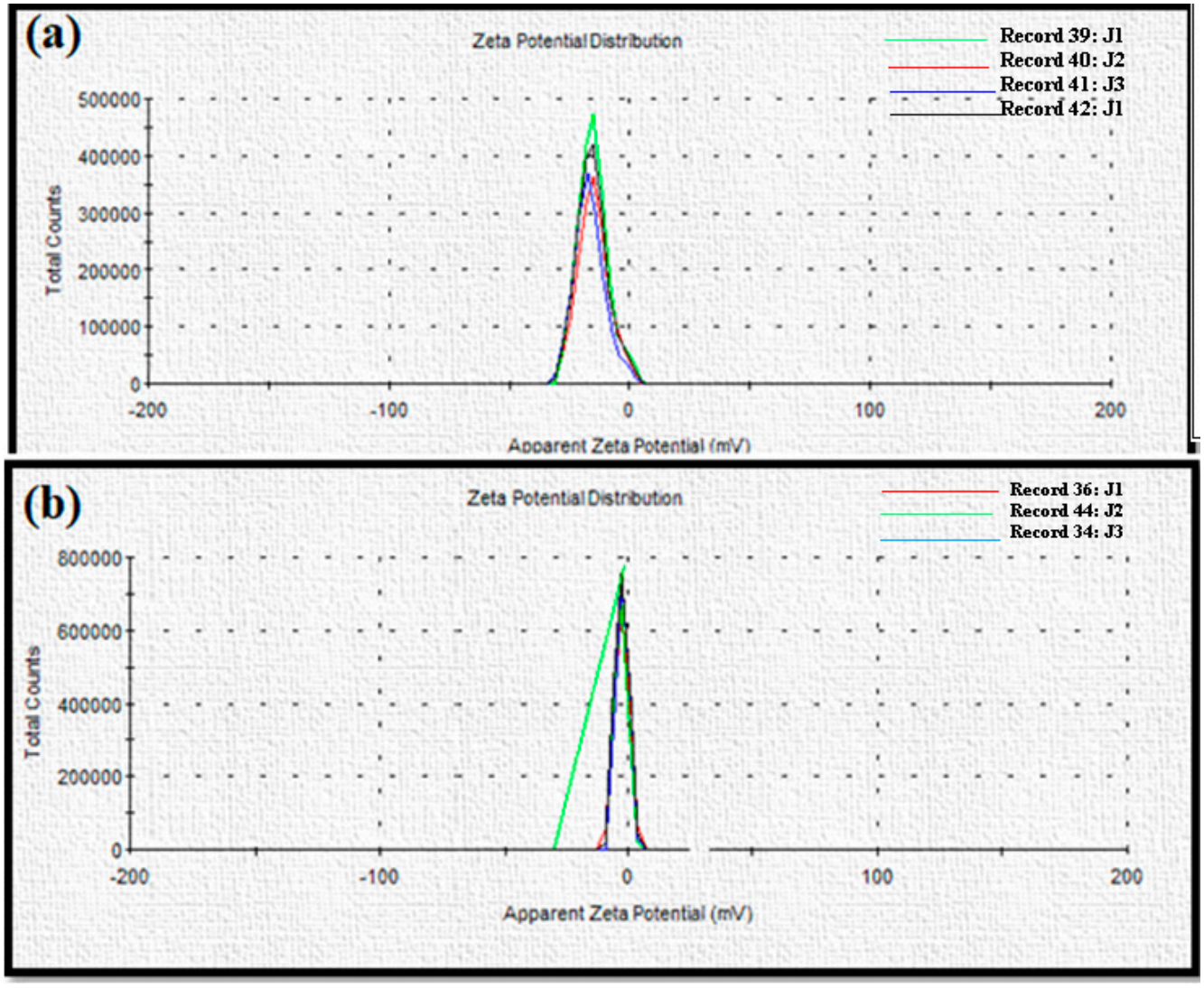

Figure 5. Zeta potential of (**a**) AgNPs (**b**) FeONPs.

EDAX analysis, which validates the presence of silver and iron as a significant metallic element, established the existence of metallic iron nanoparticles. The presence of silver and iron oxide was identified using the EDX spectrum. Using EDX, the weight percentages of silver (48.93%), iron (51.02%), oxide (39.14%), and other elements (3.14%) were calculated

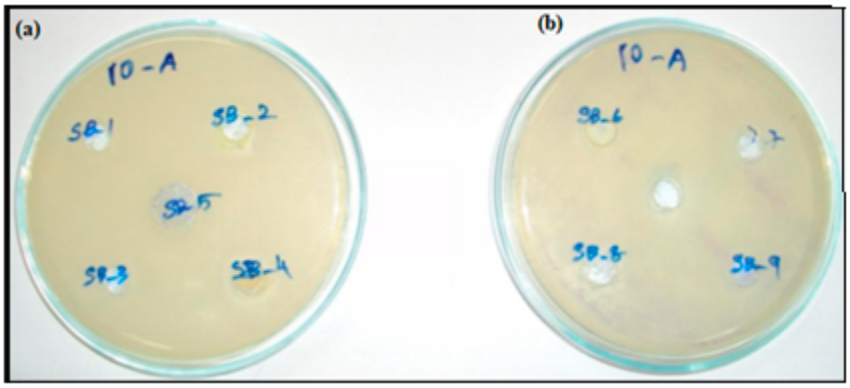

Figure 6. Antimicrobial activity of synthesized nanoparticles against *Staphylococcus aureus*, *Bacillus subtilis*, *Pseudomonas aeruginosa*, and *Escherichia coli*. (**a**) AgNPs (**b**) FeONPs.

3.4. Antimicrobial Activity

The biogenic silver and iron oxide nanoparticles acquired from the aqueous leaf extracts of *Leucas cephalotes* and *Ajuga macrosperma* were investigated for antimicrobial potential against MDR clinical bacterial isolates by utilizing the agar well diffusion method. The MDR clinical isolates of *E. coli*, *Shigella* spp., *Pseudomonas aeruginosa*, *Aeromonas* spp., and *Candida tropicalis* were susceptible to NPs. Table 1 shows that *Pseudomonas aeruginosa* was more sensitive than *Staphylococcus aureus*. Thus, the AgNPs that are created by *Leucas cephalotes* plant extract are effective on *Candida albicans* yeast. Strangely, stand-alone FeONPs (created by macrosperma) did not show antimicrobial activity.

According to antibacterial effectiveness against Gram-positive bacteria and Gram-negative bacteria, the inhibition zone's variation was recorded. Table 1 shows the values of the inhibitory zones for *Staphylococcus aureus*, *Pseudomonas aeruginosa*, *Candida albicans*, *Escherichia coli*, and *Bacillus subtilis* for both NPs which were produced by combining the leaf extracts of *Leucas cephalotes* and *Ajuga macrosperma* moreover.

3.4.1. Antimicrobial Activity of Silver Nanoparticles towards Gram-Positive Bacteria, Gram-Negative Bacteria, and Yeast

Regarding antibacterial action, the inhibition zone's variation was observed when it came to Gram-positive bacteria. Table 1 shows the values of the inhibitory zones for *Staphylococcus aureus* and *Bacillus subtilis* for AgNPs, which were made from the leaf extracts of *Leucas Cephalotes*. Additionally, it was found that the silver nanoparticles had extremely high activity against *Staphylococcus aureus*, *Pseudomonas aeruginosa*, and *Candida albicans*. However, AgNPs showed less activity towards *Bacillus subtilis* and *Escherichia coli*.

3.4.2. Antimicrobial Activity of Iron Oxide Nanoparticles towards Gram-Positive Bacteria, and Gram-Negative Bacteria, and Yeast

Regarding antibacterial action, varying inhibition zones were reported against Gram-positive bacteria. FeONPs were created by the leaf extracts of *Ajuga macrosperma*. The values of the inhibitory zones for *Staphylococcus aureus*, *Pseudomonas aeruginosa*, *E. coli*, *Candida albicann*, and *Bacillus subtilis* are shown in Table 2. Additionally, it was found that FeONPs showed high activity against *Pseudomonas aeruginosa* and *E. coli* and no activity towards *Bacillus subtilis* and *Candida albicans*.

Table 2. The IC50 of synthesized metallic nanoparticles against MCF-7 (breast cancer), HeLa, PC-3 (prostate cancer), and A549 (lungs cancer) cell lines.

S.N.	Plant Name	Nanoparticle Name	PC-3 (Prostate Cancer) IC_{50}	HeLa IC_{50}	A549 (Lung Cancer) IC_{50}	MCF-7 (Breast Cancer) IC_{50}
1.	*Abies Pindrow* Royle	FeONPs	1.23	2.0	3.98	1.91
2.	*Ajuga macrosperma*	FeONPs	2.65	4.78	8.97	1.10

Recently, *Ludwigia octovalvis* [17], *Solanum nigrum* leaves [18], *Mimusops elengi* fruit [19], *Salacia chinensis* L. [20], *Vitex negundo* [21], *Mimusops elengi*, Linn. [14], and *Laurus nobilis* extract mediated synthesized AgNPs was reported the antibacterial activity against the gram-negative and gram-positive stain [22–24].

3.5. Anticancer Activity

The synthesized AgNPs and FeONPs determined the anticancer (cytotoxicity) activity in the prostate, lung, and human breast cancer cells using MTT and MTS assay. MDA-MB-231 human breast cancer cells were also treated with different concentrations (100, 33.33, 11.11, 3.70, 1.23, and 0.41 µg/mL) of synthesized AgNPs and FeONPs. After 24 h, the treated cells were examined for changes in nuclear morphology. The cells' viability was considerably reduced in the presence of green synthesized AgNPs and FeONPs as compared with the positive/negative control. At 24 h of treatment, the IC50 values of the AgNPs were found to be ±2.11, ±2.01, and ±3.21 µg/mL for prostate (PC-3), lung (A-549), and human breast (HeLa) cancer. FeONPs were observed as ±2.65, 8.90, and 4.65 µg/mL, respectively. These results show that the minimum dose of synthesized AgNPs and FeONPs showed good cytotoxicity activity against the prostate (PC-3), lung (A-549), and human breast (HeLa) cancer cell lines (shown in Table 2). AgNPs had the highest cytotoxicity activity towards lung cancer cell lines among other cancer cell lines. Additionally it was also found that synthesized AgNPs and FeONPs determined the anticancer (cytotoxicity) activity in the human breast cancer (MCF-7) cells using MTT assay. The results show that the minimum dose of FeONPs shows excellent activity towards MCF-7 cancer cell lines. Several studies suggest that the remarkable cytotoxicity (anticancer properties) of biologically synthesized MNPs increase with the increasing concentration of NPs [25–27].

3.6. Conclusions

We synthesized silver and iron oxide nanoparticles using aqueous leaf extract of *Leucas cephalotes* and *Ajuga macrosperma* in a rapid, straightforward, economical, and environmentally-friendly manner without the involvement of hazardous chemicals. Various reaction parameters such as the concentration of extract and $AgNO_3$ and $FeSO_4$ solution, pH and reaction time, and temperature were optimized for the synthesis of AgNPs and FeONPs. The NPs were spherical and cubic in shape with a particle size of 10 to 30 nm and negative zeta potential of −23.36, and −27.06 mV.

The NPs were stable over a period of 10 d at room temperature, and demonstrated antimicrobial and anticancer properties. The biosynthesized AgNPs and FeONPs showed in vitro anticancer activity in breast cancer (MCF-7 and HeLa), prostate cancer (PC-3), and lung (A-549) cancer cell lines. The biosynthesized AgNPs and FeONPs also showed good antimicrobial activity against five pathogenic microbes (*Staphylococcus aureus*, *Bacillus subtilis*, *Pseudomonas aeruginosa*, and *Escherichia coli*). The AgNPs could be further explored as therapeutic agents in the treatment of cancer.

Author Contributions: S.P. and A.K. wrote the main manuscript text; V.G. and V.N.K. prepared different tables and figures. All authors reviewed the manuscript. All authors have read and agreed to the published version of the manuscript.

Funding: This research received no external funding.

Institutional Review Board Statement: Not applicable.

Informed Consent Statement: Not applicable.

Data Availability Statement: All data generated during this study are included in this published article.

Conflicts of Interest: The authors declare no conflict of interest. The authors declare that they have no known competing financial interests or personal relationships that could have appeared to influence the work reported in this paper.

References

1. Abalkhil, T.A.; Alharbi, S.A.; Salmen, S.H.; Wainwright, M. Bactericidal activity of biosynthesized silver nanoparticles against human pathogenic bacteria. *Biotechnol. Biotechnol. Equip.* **2017**, *31*, 411–417. [CrossRef]
2. Munita, J.M.; Arias, C.A. Mechanisms of antibiotic resistance. *Microbiol. Spectr.* **2016**, *4*, 481–511. [CrossRef] [PubMed]
3. Mansoori, B.; Mohammadi, A.; Davudian, S.; Shirjang, S.; Baradaran, B. The different mechanisms of cancer drug resistance: A brief review. *Adv. Pharm. Bull.* **2017**, *7*, 339.
4. Nile, A.; Nile, S.H.; Shin, J.; Park, G.; Oh, J.W. Quercetin-3-glucoside extracted from apple pomace induces cell cycle arrest and apoptosis by increasing intracellular ROS levels. *Int. J. Mol. Sci.* **2021**, *22*, 10749. [CrossRef] [PubMed]
5. Siddiqi, K.S.; Husen, A.; Rao, R.A. A review on biosynthesis of silver nanoparticles and their biocidal properties. *J. Nanobiotechnol.* **2018**, *16*, 14.
6. Patel, S.K.; Kalia, V.C. Advancements in the nanobiotechnological applications. *Indian J. Microbiol.* **2021**, *61*, 401–403. [CrossRef]
7. Nakamura, S.; Sato, M.; Sato, Y.; Ando, N.; Takayama, T.; Fujita, M.; Ishihara, M. Synthesis and application of silver nanoparticles (Ag NPs) for the prevention of infection in healthcare workers. *Int. J. Mol. Sci.* **2019**, *20*, 3620. [CrossRef]
8. Hosseini-Koupaei, M.; Shareghi, B.; Saboury, A.A.; Davar, F.; Sirotkin, V.A.; Hosseini-Koupaei, M.H.; Enteshari, Z. Catalytic activity, structure and stability of proteinase K in the presence of biosynthesized CuO nanoparticles. *Int. J. Biol. Macromol.* **2019**, *122*, 732–744. [CrossRef]
9. Tavakoli, S.; Kharaziha, M.; Ahmadi, S. Green synthesis and morphology dependent antibacterial activity of copper oxide nanoparticles. *J. Nanostructures* **2019**, *9*, 163–171.
10. Berra, D.; Laouini, S.E.; Benhaoua, B.; Ouahrani, M.R.; Berrani, D.; Rahal, A. Green synthesis of copper oxide nanoparticles by Pheonix dactylifera L leaves extract. *Dig. J. Nanomater. Biostruct.* **2018**, *13*, 1231–1238.
11. Nile, S.H.; Baskar, V.; Selvaraj, D.; Nile, A.; Xiao, J.; Kai, G. Nanotechnologies in food science: Applications, recent trends, and future perspectives. *Nano-Micro Lett.* **2020**, *12*, 45. [CrossRef]
12. Díaz, M.; Barba, F.; Miranda, M.; Guitián, F.; Torrecillas, R.; Moya, J.S. Synthesis and antimicrobial activity of a silver-hydroxyapatite nanocomposite. *J. Nanomater.* **2009**, *2009*, 498505.
13. Kumar, K.M.; Mandal, B.K. Speciation of green iron nanoparticles in situ by a simple UV-Visible technique. *J. Indian Cdhemidcal Soc.* **2012**, *89*, 1653–1658.
14. Prakash, P.; Gnanaprakasam, P.; Emmanuel, R.; Arokiyaraj, S.; Saravanan, M. Green synthesis of silver nanoparticles from leaf extract of *Mimusops elengi*, Linn. for enhanced antibacterial activity against multi drug resistant clinical isolates. *Colloids Surf. B Biointerfaces* **2013**, *108*, 255–259. [CrossRef] [PubMed]
15. Abid, M.A.; Kadhim, D.A.; Aziz, W.J. Iron oxide nanoparticle synthesis using trigonella and tomato extracts and their antibacterial activity. *Mater. Technol.* **2022**, *37*, 547–554.
16. Sayed, F.N.; Polshettiwar, V. Facile and sustainable synthesis of shaped iron oxide nanoparticles: Effect of iron precursor salts on the shapes of iron oxides. *Sci. Rep.* **2015**, *5*, 9733. [CrossRef] [PubMed]
17. Sarathi Kannan, D.; Mahboob, S.; Al-Ghanim, K.A.; Venkatachalam, P. Antibacterial, antibiofilm and photocatalytic activities of biogenic silver nanoparticles from *Ludwigia octovalvis*. *J. Clust. Sci.* **2021**, *32*, 255–264. [CrossRef]
18. Jenifer, A.A.; Malaikozhundan, B.; Vijayakumar, S.; Anjugam, M.; Iswarya, A.; Vaseeharan, B. Green synthesis and characterization of silver nanoparticles (AgNPs) using leaf extract of Solanum nigrum and assessment of toxicity in vertebrate and invertebrate aquatic animals. *J. Clust. Sci.* **2020**, *31*, 989–1002. [CrossRef]
19. Korkmaz, N.; Ceylan, Y.; Hamid, A.; Karadağ, A.; Bülbül, A.S.; Aftab, M.N.; Çevik, Ö.; Şen, F. Biogenic silver nanoparticles synthesized via Mimusops elengi fruit extract, a study on antibiofilm, antibacterial, and anticancer activities. *J. Drug Deliv. Sci. Technol.* **2020**, *59*, 101864. [CrossRef]
20. Nagesh, M.R.; Kumar, N.; Khan, J.M.; Ahmed, M.Z.; Kavitha, R.; Kim, S.J.; Vijayakumar, N. Green synthesis and pharmacological applications of silver nanoparticles using ethanolic extract of *Salacia chinensis* L. *J. King Saud Univ.-Sci.* **2022**, *34*, 102284. [CrossRef]
21. Dogra, S.; Sharma, M.D.; Tabassum, S.; Mishra, P.; Bhatt, A.K.; Bhuyar, P. Green biosynthesis of silver nanoparticles (agnps) from vitex negundo plant extract and its phytochemical screening and antimicrobial assessment next to pathogenic microbes. *J. Microbiol. Biotechnol. Food Sci.* **2023**, *12*, 1–7.
22. Al-Ghamdi, A.Y. Antimicrobial and catalytic activities of green synthesized silver nanoparticles using bay laurel (*Laurus nobilis*) leaves extract. *J. Biomater. Nanobiotechnol.* **2019**, *10*, 26–39.

23. Chandrasekar, N.; Kumar, K.; Balasubramnian, K.S.; Karunamurthy, K.; Varadharajan, R. Facile synthesis of iron oxide, iron-cobalt and zero valent iron nanoparticles and evaluation of their anti microbial activity, free radicle scavenginging activity and antioxidant assay. *Dig. J. Nanomater. Biostruct. DJNB* **2013**, *8*, 765–775.
24. Krishnaraj, C.; Muthukumaran, P.; Ramachandran, R.; Balakumaran, M.D.; Kalaichelvan, P.T. Acalypha indica Linn: Biogenic synthesis of silver and gold nanoparticles and their cytotoxic effects against MDA-MB-231, human breast cancer cells. *Biotechnol. Rep.* **2014**, *4*, 42–49.
25. Liu, H.; Shi, W.; Luo, Y.; Cui, G.; Kong, X.; Han, L.; Zhao, L. Green supported of Au nanoparticles over reduced graphene oxide: Investigation of its cytotoxicity, antioxidant and anti-human breast cancer properties. *Inorg. Chem. Commun.* **2021**, *134*, 108918. [CrossRef]
26. Biresaw, S.S.; Taneja, P. Copper nanoparticles green synthesis and characterization as anticancer potential in breast cancer cells (MCF7) derived from Prunus nepalensis phytochemicals. *Mater. Today Proc.* **2022**, *49*, 3501–3509. [CrossRef]
27. Banerjee, S.; Islam, S.; Chattopadhyay, A.; Sen, A.; Kar, P. Synthesis of silver nanoparticles using underutilized fruit *Baccaurea ramiflora* (Latka) juice and its biological and cytotoxic efficacy against MCF-7 and MDA-MB 231 cancer cell lines. *S. Afr. J. Bot.* **2022**, *145*, 228–235. [CrossRef]

Disclaimer/Publisher's Note: The statements, opinions and data contained in all publications are solely those of the individual author(s) and contributor(s) and not of MDPI and/or the editor(s). MDPI and/or the editor(s) disclaim responsibility for any injury to people or property resulting from any ideas, methods, instructions or products referred to in the content.